RESEARCH PAPER

PCCP
www.rsc.org/pccp

# The pH dependent adsorption of Coumarin 343 at the water/dichloroethane interface

**Debi Pant,[a] Mireille Le Guennec,[b] Bertrand Illien[b] and Hubert H. Girault*[a]**

[a] *Laboratoire d'Electrochimie, Ecole Polytechnique Fédérale de Lausanne, CH 1015 Lausanne, Switzerland. E-mail: Hubert.Girault@epfl.ch*

[b] *Laboratoire de Spectrochimie et Modélisation, EA 1149-FR CNRS 2465, Faculté des Sciences et Techniques, 2, rue de la Houssinère, BP 92208 F-44322, Nantes Cédex 3, France*

***Received 22nd March 2004, Accepted 27th April 2004***
***First published as an Advance Article on the web 17th May 2004***



The surface sensitive technique of optical second harmonic generation (SHG) and quasi-elastic laser scattering (QELS) have been applied to study the effect of pH on the adsorption of Coumarin 343 (C343) dye molecules at the water/1, 2-dichloroethane (DCE) interface. A pH dependent aggregation is observed for C343 molecules adsorbed at the interface. The surface spectrum shows that at pH 8 and lower, C343 adsorb at the interface in J-aggregated protonated form. At pH 9 and pH 10, C343 adsorb in both protonated and deprotonated forms at the interface, whereas, at pH 11, C343 is in H-aggregated-deprotonated form at the interface. The observed large shift in p$K_a$ value of C343 at the interface is attributed to the intramolecular hydrogen bonding along with the aggregation of dye molecules. From a light polarization analysis of the SHG signal, the average angle of orientation of C343 at pH 5 was determined to be 30°, and at pH 11, the angle was determined to be 42°. The QELS data show a weak adsorption of C343 at the interface for pH 11 and pH 3 and a strong adsorption at the intermediate pH values, reaching maximum for pH 10, and are consistent with SHG data. The calculated ratio of $\beta$ values for protonated and deprotonated forms of C343, is in agreement with the experimentally measured ratio of $\beta$ values. Both, experimental and calculated $\beta$ values for the deprotonated form is lower than the $\beta$ values for protonated one and is attributed to the electron-donating effect of the $-COO^-$ substituent.

## 1. Introduction

Knowledge of interfacial acid–base properties is important in understanding the molecular properties and chemical reactions at the interfaces. Experimentally, it has already been demonstrated that the acid–base equilibrium constants are different at interfaces from that in bulk solutions.[1–5] Shen and coworkers[1] have demonstrated that second harmonic generation (SHG) technique is capable of measuring the proton excess at the air/water interfaces. From SHG measurements, Eisenthal and co workers[2] have determined the p$K_a$ of *p*-hexadecyl aniline at the air/water interface. They observed that the p$K_a$ at the interface was 3.6 versus 5.3 in the bulk. For $CH_3(CH_2)_{21}NH_3^+$ at air/water they determined p$K_a$ of 9.9 versus 10.6 in bulk water.[3] They attributed this increase in acidity to the higher free energy of a charged species at the interface, which favors a shift in the equilibrium towards the neutral form. The surface density and electrolyte concentration dependence of p$K_a$ of $CH_3(CH_2)_{21}NH_3^+$ yielded p$K_a$ values ranging from 10.2 to 8.2 as the interface density varies from 100 to 22 Å$^2$/molecule.[4]

The acid–base equilibria have also been studied at the liquid/liquid interfaces. Corn and coworkers[5,6] have measured the adsorption of azobenzene surfactant at an aqueous pH of 8 or greater. The concentration and pH dependence of the resonant SHG from the adsorbed monolayer indicated that the surfactant was in its anionic form at the interface. As a function of pH, no change in the angle of orientation of molecule was found at the interface.

In the past we have studied eosin at the air/water interface[7] as a function of pH. We have been able to follow the appearance and disappearance of three different species of eosin at the interface as a function of aqueous bulk pH. The surface p$K_a$ values were found to be shifted to larger values as compared to the aqueous bulk solution p$K_a$. The interfacial orientation for the doubly charged and neutral forms of eosin B was found to be 33° and 31°, respectively.

Coumarin doped polymers are being extensively studied for use in non-linear optical applications such as in optoelectronic devices,[8] frequency doubling[9] of laser beam and photorefractive devices.[10] Thus it is important to study the nonlinear optical properties of bulk coumarins. In this regard, Moylan[11] has already studied the molecular hyperpolarizabilities of different coumarins, using the electric field induced second harmonic (EFISH) technique, and the hyperpolarizability value measured for C343 (Fig. 1) was $29 \times 10^{-30}$ esu. In this paper we report the effect of pH on the adsorption of C343 at the water/DCE interface using SHG and quasi-elastic laser scattering (QELS) techniques. The surface spectrum shows complex pH dependent adsorption at the water/DCE interface. The QELS measurements as a function of pH are fully compatible with the SHG data. The theoretical calculations for the ratio of hyperpolarizability values for protonated and deprotonated forms of dye is in reasonable agreement with the experimentally measured value.

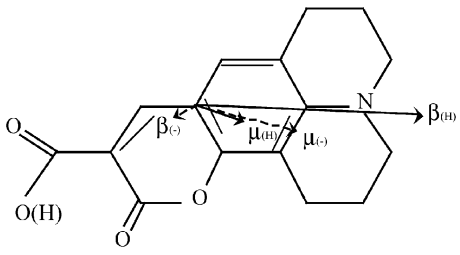


**Fig. 1** Structure of C343, and directions of the AM1 ground-state dipole moment and of the vector part of the $\beta$ (0) tensor for the protonated (H) and deprotonated (−) forms of C343.

DOI: 10.1039/b404329d

 

## 2. Experimental

The optical setup for SHG measurements have been described in detail.[12,13] The fundamental beam at frequency $\omega$ is provided by an optical parametric oscillator (OPO) (Spectra-Physics MOPO 710) pumped with the third harmonic of a Q-switched $Nd^{3+}$:YAG laser. The fundamental wavelength was tuned from 760 to 1400 nm. Pulses at the repetition rate of 10 Hz with 5 ns duration were delivered by the laser source. The fundamental beam was impinging at the water/DCE interface under the total internal reflection (TIR) condition with an angle of about 70°. The TIR configuration greatly enhances the intensity of the second harmonic (SH) signal from the interface. The energy per pulse at the fundamental frequency $\omega$ at the interface was about 2.8 mJ at 900 nm. The SH signal at the frequency $2\omega$ generated at the interface was detected by a photomultiplier tube through a monochromator after passing through band pass filters to cut the fundamental beam. The data were finally acquired with a boxcar integrator. To take into account the wavelength dependence of the fundamental beam energy, about 2% of the output from the OPO was split off by a beam splitter and detected by a power meter. The collected SH signal was normalized by dividing the SH intensity by the square of the laser energy. The fundamental beam was s-polarized unless otherwise mentioned. The polarization measurements to estimate the orientation parameters of the interfacial species were achieved by rotating the fundamental polarization with an achromatic half wave plate.

The experimental setup for QELS measurements is described in detail previously.[14] The laser used was a cw He–Ne laser delivering 4 mW at 632.8 nm. The diffraction grating used consist dark lines with 0.285 mm spacing prepared on a photographic glass plate. The optical beat of third order diffraction spot was monitored by a photomultiplier tube and was analyzed by a fast-Fourier transform (FFT) analyzer (Stanford Research Systems SR770). The optical cell was a cylindrical glass cell with an interfacial area of 15.9 $cm^2$. The water surface was covered with the optical glass window to minimize light scattering from the water/air interface.

Water was purified by reverse osmosis followed by ion exchange (Millipore, Milli-Q SP regent system). The 1,2-dichloroethane (Merck, extra pure), and C343 (Aldrich) were used as received. The C343 dye is dissolved in aqueous phase unless otherwise mentioned. The pH of the solution was adjusted by using HCl for lower pH and NaOH for higher pH. At very low pH values such as at pH = 3, the solubility of the dye molecules in the water phase decreases rapidly and the diffusion of dye molecules from the water phase to the organic phase takes place. All the experimental measurements were done with the freshly prepared solutions.

## 3. Results and discussion

### 3.1 Linear and non-linear optical measurements

The second harmonic (SH) intensity at frequency $2\omega$ under TIR conditions can be expressed by the equation[15]

$$I^{2\omega} = \frac{\omega^2}{8\varepsilon_0 c^3} \frac{\sqrt{\varepsilon_1^{2\omega}}}{\varepsilon_1^{\omega}\left(\varepsilon_m^{2\omega} - \varepsilon_1^{\omega}\sin^2\theta_1^{\omega}\right)} |\chi|^2 (I^{\omega})^2 \qquad (1)$$

where $\varepsilon$ and $\theta$ are the relative dielectric constant and the angle of incidence of the fundamental beam. The subscripts 1 and m relate to the incident medium and the interface, respectively. The relative dielectric constant of the interface ($\varepsilon_m$) can be taken as the mean value between the two bulk media as reported by recent surface SHG studies.[16] For an isotropic surface or interface such as the water/DCE, the macroscopic quantity ($\chi$) is a function of three nonzero elements of the second order surface susceptibility tensor ($\chi_S$)

$$\chi = a_1\chi^2_{S,XZX}\sin 2\gamma\sin\Gamma + \left(a_2\chi^2_{S,XZX} + a_3\chi^2_{S,ZZZ} + a_4\chi^2_{S,ZZZ}\right) \times \cos^2\gamma\cos\Gamma + a_5\chi^2_{S,ZXX}\sin^2\gamma\cos\Gamma \qquad (2)$$

where $\gamma$ and $\Gamma$ are the angle of polarization of the fundamental and the harmonic waves. The optical coefficients $a_1$–$a_5$ are determined from the relative dielectric constants of the different media and the angle of incidence. Finally, the macroscopic susceptibility tensor $\chi_S$ is related to the molecular quantities. It is the product of the total number of optically nonlinear active molecules adsorbed at the interface per unit surface $N_S$ and the molecular hyperpolarizability, $\beta$ of a single moiety.[17]

$$\chi^2_S = \frac{N_S}{\varepsilon_0}\langle\beta\rangle \qquad (3)$$

where the $\beta$ tensor is taken as an ensemble average over all the possible orientation configurations.

UV-visible spectra of C343 in bulk aqueous (pH = 7) and bulk DCE are presented in Fig. 2 along with the corresponding SHG spectrum at the water/DCE interface. In bulk aqueous solutions the absorption maximum of C343 is at 428 nm and is in agreement with the reported values.[18] In bulk DCE solution, the absorption spectrum of C343 is red shifted and the maximum is at 450 nm. The surface spectrum of C343 at the water/DCE interface is further red shifted from the bulk DCE absorption spectrum and the maximum is around 470 nm. On dissolving C343 in DCE phase, no change in the peak position (470 nm) and shape of the surface spectrum is observed on comparing it with the surface spectrum obtained on dissolving C343 in water phase. In both the cases, the surface spectra are much narrower than the corresponding absorption spectra. This observation clearly indicates that the observed spectra are due to the nonlinear optical process at the interface, and the interfacial properties are the same in both the cases.

We measured the surface spectrum of C343 at the water/DCE interface as a function of dye concentration (Fig. 3). We observed a slight red shift (6 nm) in the peak position on varying the dye concentration from 50 nM to 0.2 mM. Beyond 0.2 mM, no further shift in the surface spectrum was observed with the increase of dye concentration. The spectral shape remains unchanged up to 30 μM, but above this concentration

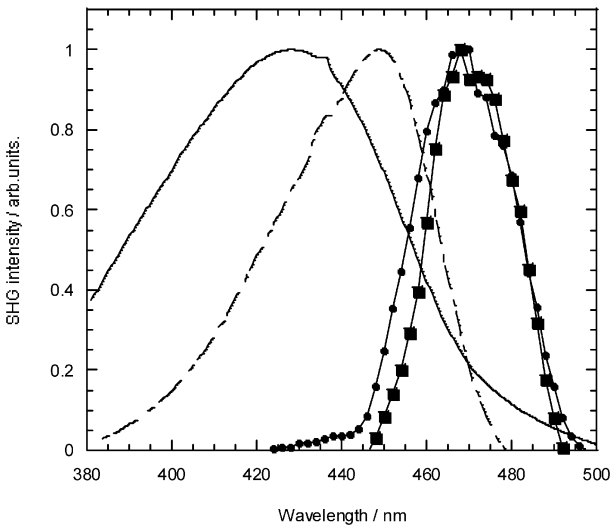


**Fig. 2** UV-Visible absorption spectra of C343 in aqueous solution (solid line) and in DCE (dashed dotted line), and surface SHG spectrum at the water/DCE interface on dissolving C343 in aqueous phase (filled circles), on dissolving C343 in organic phase (filled squares).

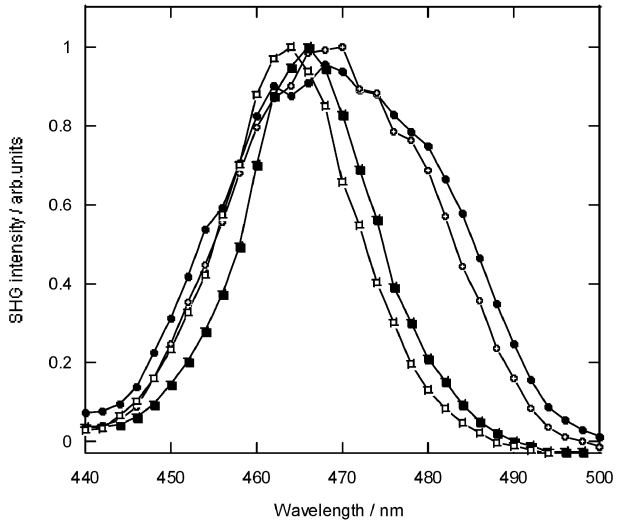


**Fig. 3** Concentration dependence of surface SHG spectrum of C343 at water/DCE interface. 200 μM (filled circles), 40 μM (open circles), 30 μM (filled squares), 100 nM (open squares).

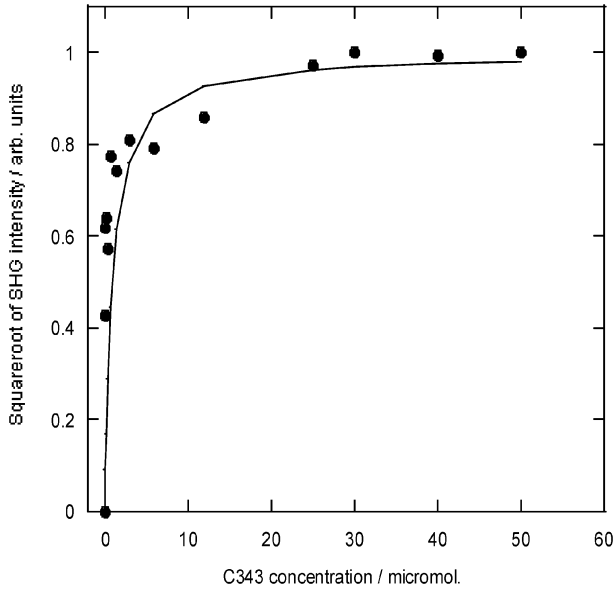


**Fig. 4** The Adsorption isotherm of C343 (filled circles) at the water/DCE interface. The solid line fits to the isotherm of the form of eqn. (4). The bulk aqueous pH = 8.

a change in the FWHM is observed with the increase in concentration of the dye molecule. The shift in the surface spectrum and change in the shape of the surface spectrum with the concentration of dye are the clear indications of aggregation of the dye molecules at the interface.

The observed red shift in the surface spectrum of about 40 nm from the bulk aqueous absorption spectrum and about 20 nm from the bulk DCE can be explained by different possible arguments. First, the red shift observed in surface spectrum may be simply due to the weaker polarity at the interface.[16] Second, strong interactions among the closely packed dye molecules at the interface could result a red shift in the spectrum. However, the adsorption isotherm we have studied for C343 molecules in the next section follows a simple Langmuir adsorption isotherm which indicates that the interactions of the adsorbed dye molecules at the interface are not very strong. Third, the red shift in surface spectrum could be due to the protonation of dye at the interface. There are reports[18,19] in the literature about the shift of peak position of the absorption spectrum of bulk C343 from 428 nm in neutral or basic solution to 456 nm in acidic solution, and this red shift in absorption spectrum has been attributed to the protonation of the dye molecule in the acidic solution. There are several sites on the C343 molecule that could potentially accept a proton, the carboxylic acid group, the cyclic ester and cyclic amine moieties. Riter *et al.*[18] observed that for the lower values of pH, C343 molecules get protonated on the carboxylic acid moiety. Fourth, the red shift could be simply due to the aggregation of dye molecules at the interface. Aggregation of C343 dye molecules has been observed for the molecules adsorbed at the surfaces of nanoparticles.[20] The absorption spectra of C343 attached with $ZrO_2$ nanoparticles showed a dramatic change with the dye concentration. The observed large blue shift in the absorption spectra with the dye concentration has been attributed to the H-aggregation of the dye molecules at the surface.[20]

### 3.2 Adsorption isotherm of C343

In order to determine the adsorption properties, the SHG intensity was monitored as a function of bulk aqueous concentration of C343. As it is clear from eqns. (1)–(3), the SHG signal from the interface is proportional to the square of the number of molecules adsorbed per unit surface $N_S$ or to the square of the surface coverage, and hence the plot of square root of SH intensity against the concentration of C343 yield the adsorption isotherm of the molecule. Fig. 4 shows the adsorption isotherm of C343 at neat water/DCE interface. The measurements were performed at 470 nm with both the fundamental and second harmonic waves p-polarized. The bulk aqueous concentration was varied from zero to 0.2 mM. The full monolayer coverage was obtained at a bulk aqueous concentration of about 30 μM.

The adsorption isotherm shown in Fig. 4 exhibits a simple Langmuir isotherm behavior indicating that there are no strong interactions between the species adsorbed at the interface. The flattening occurring of the isotherm curve above 30 μM is the characteristic of the full monolayer coverage. The SHG response was observed for the concentrations as low as 50 nM. The fit of the data to the following Langmuir isotherm expression

$$\frac{N_S}{N_S^{max}} = \frac{a^w \exp(-\Delta G/RT)}{1 + a^w \exp(-\Delta G/RT)} \qquad (4)$$

yielded the value −32 kJ $mol^{-1}$ for the Gibbs energy of adsorption. This value is similar to the values reported for other molecules adsorbed at the liquid/liquid interface.[13]

### 3.3 Effect of pH on surface spectrum of C343

We investigated the effect of the bulk pH on the SHG spectra of C343 at water/DCE interface. The SHG spectrum of C343 at water/DCE interface is presented in Fig. 5 for different pH values. From pH 3 to pH 8, there is no change in the shape of surface spectrum and the peak position of the spectrum is at 470 nm. At pH 9, the surface spectrum shifts to the blue with broadening in the spectrum. The shape of the spectrum also changes, having two distinct peaks and two other shoulders. The observed two peak positions at 450 nm and 430 nm in the surface spectrum correspond to the absorption spectrum of bulk C343. in protonated and deprotonated forms,[18,19] respectively. On further increasing the pH, the peak corresponding to the deprotonated form (430 nm) becomes stronger than the peak corresponding to the DCE (450 nm). At pH 11, the width of the surface spectrum narrows down and the peak position of spectrum is around 410 nm and a shoulder around 430 nm. Beyond pH 11, the dye solutions chemically degrade and no measurements have been done. A continuous increase in SHG intensity is observed with the increase in pH of the solution from pH 3 to pH 10. However, a sudden decrease is observed in

 

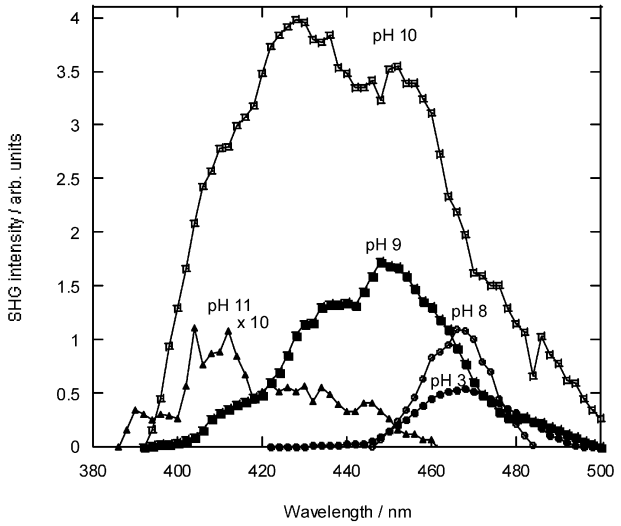


**Fig. 5** The pH dependence of surface spectrum of C343 (30 μM) at water/DCE interface, pH 11 (filled triangles), pH 10 (open squares), pH 9 (filled squares), pH 8 (open circles), pH 3 (filled circles).

the intensity of SHG signal at pH 11. The second harmonic intensity at the maximum of the surface spectrum for pH 11 is about ten times less than the intensity at pH 5.

We believe that the surface spectrum for pH 8 and lower arise from the aggregated protonated form of the dye at the interface. The maximum of the absorption spectrum of the protonated form of C343 dye is around 456 nm.[19] However, the maximum of the surface spectrum, we have measured here is around 470 nm. We attribute this 15 nm further red shift in the surface spectrum from the absorption spectrum of the protonated form of C343 to the J-aggregation of dye molecules at the interface. J-aggregates are formed when the dye molecules arrange themselves head-to-tail in a slanted stack.[21] For these aggregates the allowed absorption band is observed at lower energy than the monomer absorption band. At pH 9, the peak around 450 nm is attributed to the non-aggregated protonated form, whereas, the shoulder around 470 nm is due to the J-aggregated protonated form of the dye at the interface. The peak around 430 nm is attributed to the non-aggregated deprotonated form of the dye, whereas, the shoulder around 410 nm is due to the H-aggregated deprotonated form of the dye. At pH 10, an increase in SH intensity around 430 nm and a decrease around 450 nm clearly indicate that the deprotonated form of the dye molecules dominate the interfacial concentration over the protonated form of the dye. At pH 11, the surface spectrum arises only from the deprotonated form of the dye. The peak around 430 nm is due to the deprotonated form, whereas, a peak around 410 nm is due to H-aggregated deprotonated form of the dye at the interface. H-aggregates are formed when the dye molecules arrange parallel in a vertical stack.[21] For these aggregates the allowed absorption band is observed at higher energy than the monomer absorption band.

The above discussed data of surface spectrum clearly show that the behavior of adsorption of C343 at water/DCE interface as a function of pH is quite complicated, and precludes us from the exact determination of p$K_a$ value of C343 at the interface. The p$K_a$ value reported for C343 in bulk solutions is 4.65.[18] However, the observation that the surface spectrum remains unchanged for pH values lower than pH 8 and changes in peak position and in shape on further increase in pH clearly indicates that the p$K_a$ of C343 is shifted by several units at the interface compared to the bulk p$K_a$ value, and p$K_a$ value is certainly more than p$K_a$ = 8 at the interface. There are several reports in the literature about the shift in p$K_a$ values at the interfaces[3,4,22–25] compared to the bulk solutions. For several acid/base indicators,[22,23] the differences in the p$K_a$ values at the interfaces of the micelles compared to the bulk water solutions is generally ascribed to the probe molecules residing in a lower dielectric environment at the interface than in the bulk water. In the case of simple molecules, the shift in p$K_a$ values at the interfaces is about 1–2 units only,[3,4] whereas, a large shift in p$K_a$ values, as much as by five units is observed for 4-octadecyloxy-1-naphthoic acid (ONA)[24,25] in air-water films. The observed high p$K_a$ values of ONA in micellar solutions and in monolayer films adsorbed onto silica plates studied by conventional UV absorption and fluorescence methods has been attributed to the ONA aggregation at the interfaces. The theoretical calculations performed for the protonated form of C343 (section 3.6) have shown that the hydrogen on the carbonyl group forms an intramolecular hydrogen bond with the nearby carbonyl group. We assume that the strong intramolecular hydrogen bonding facilitates the extensive aggregation of C343 molecules at the interface. Consequently, in the same way as for ONA molecules,[25] the observed large shift in the p$K_a$ value of C343 at the interface compared to the bulk aqueous solution can be attributed to the strong intramolecular hydrogen bonding along with the aggregation of dye molecules.

### 3.4 Light polarization measurements for C343

The orientation of the molecules at the interface can be obtained from the light polarization analysis of SH intensity. The s and p curves for C343 at water/DCE are not very different from each other except an overall difference in

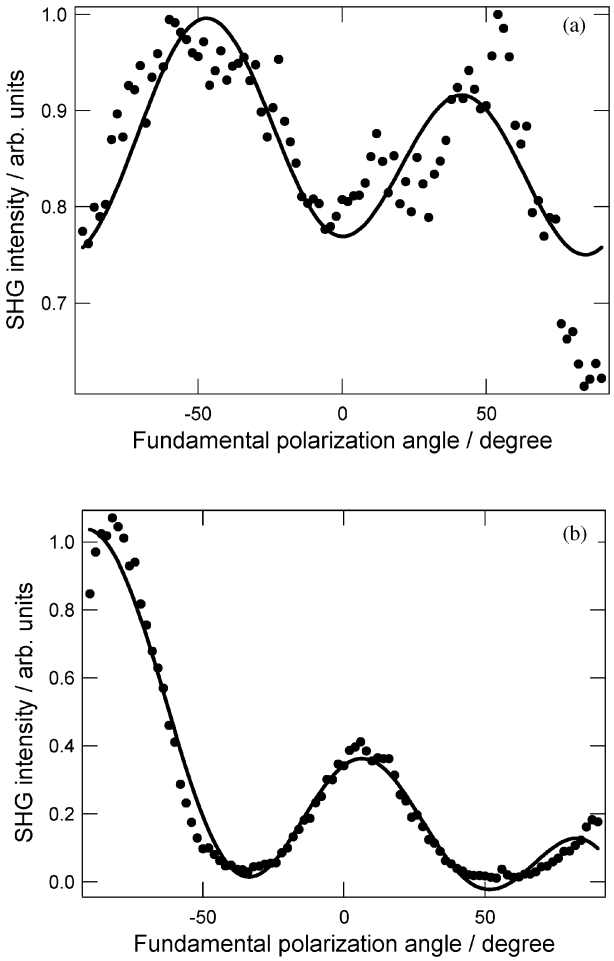


**Fig. 6** Polarization curves for C343 (30 μM) at water/DCE interface. (a) pH 11 at 415 nm, (b) pH 5 at 470 nm. The beam at the second harmonic wavelength is p-polarized. Filled circles are the SHG data and the solid lines are fits to eqns. (1) and (2).

intensities. Fig. 6 shows the p-polarization curves as a function of fundamental polarization angle for C343 at pH 5 and pH 11. The polarization curves at pH 5 and pH 11 are different from each other indicating that the orientation of the adsorbed molecules at the interface is different for different pH values of the solution. In order to estimate the angle of molecular orientation, the s- and p-polarized output curves were analyzed by using eqns. (1) and (2) and the values of three independent tensor elements $\chi_{s,XZX}$, $\chi_{s,ZXX}$ and $\chi_{s,ZZZ}$ have been obtained for pH 5 and pH 11. As the molecular point group of C343 is $C_1$, describing the C343 molecule the same way as Coumarin 314,[26] the $z$-axis of C343 molecule (Fig. 1) can be taken along the direction of transition dipole moment and is considered as the reference axis of rotation. The benzene rings of the molecule are located at the $xz$-plane. The $x$-axis is taken perpendicular to the $z$-axis in the plane of the ring. The $y$-axis is taken perpendicular to the ring and no delocalization is considered in this direction, hence no contribution occurs in this direction and therefore all tensor elements with a $y$ index vanish altogether. Only three independent tensor elements remain which contribute to the SH response.[15] Further, note that we have used surface tensor elements, neglecting the contributions arising from the nonlocal effects to the SH intensity. Defining the interface as the $XY$ plane, and assuming that the two nonzero elements of the molecular hyperpolarizability tensor elements $\beta_{xzx}$ and $\beta_{zzz}$ are dominant, the eqn. (3) can further be developed under these conditions, yielding[15]

$$\chi_{XZX} = \frac{N_S}{2\varepsilon_0}\left[\langle \sin^2\theta\cos\theta\rangle\beta_{ZZZ} + \langle\cos\theta\rangle\beta_{XZX}\right] \quad (5)$$

$$\chi_{ZXX} = \frac{N_S}{2\varepsilon_0}\left[\langle \sin^2\theta\cos\theta\rangle\beta_{ZZZ}\right] \quad (6)$$

$$\chi_{ZZZ} = \frac{N_S}{\varepsilon_0}\left[\langle \cos^3\theta\rangle\beta_{ZZZ}\right] \quad (7)$$

From these sets of equations, the ratio of two nonzero elements $(\beta_{zzz}^2/\beta_{xzx}^2)$ is calculated with equation

$$\frac{\beta_{zzz}^2}{\beta_{xzx}^2} = \frac{\chi_{S,ZZZ}^2 + 2\chi_{S,ZXX}^2}{2(\chi_{S,XZX}^2 - \chi_{S,ZXX}^2)} \quad (8)$$

For the measurements done at pH 5 and pH 11, the values of $(\beta_{zzz}^2/\beta_{xzx}^2)$ are approximately constant, *i.e.,* the average is 0.37. The value smaller than unity indicates that the contribution of $\beta_{xzx}^2$ is effectively larger than $\beta_{zzz}^2$. The orientation parameter (D) was calculated using equation

$$D = \frac{2\chi_{S,XZX}^2 - 2\chi_{S,ZXX}^2 - \chi_{S,ZZZ}^2}{2\chi_{S,XZX}^2 - 4\chi_{S,ZXX}^2 - \chi_{S,ZZZ}^2} \quad (9)$$

The average value of $D$ was found to be 0.74 for pH 5 and 0.55 for pH 11. The average orientation angle $\theta$ has been calculated using the equation

$$D = \frac{\langle\cos^3\theta\rangle}{\langle\cos\theta\rangle} \quad (10)$$

The calculated angle of orientation depends on the width of the angle distribution. Here a Dirac delta distribution is assumed. The average values of $\theta$ determined in this manner are 30° for pH 5 and 42° for pH 11, and are the angles between the molecular $z$-axis and the normal to the interface. The angles of orientation thus estimated suggest that the dye molecules at pH 11 are flatter to the interface than the molecules at pH 5.

The molecular hyperpolarizability, $\beta$, can be estimated using eqn. (3). The above presented polarization data are measured for the 30 μM concentration of dye molecules, and the adsorption isotherm we studied showed that at this concentration a full monolayer coverage of C343 molecules is achieved. The surface density, $N_S$, at full monolayer coverage can be estimated from the size of C343 molecule. On the basis of crystallographic data,[26] the C343 molecule is approximately $9 \times 4 \times 2$ Å$^3$. The surface occupied by a single molecule at the interface can be taken to be 0.36 nm$^2$ and thus $N_S$ is $3 \times 10^{18}$ molecules m$^{-2}$. The average susceptibility values from the above polarization data are 1.52 and 0.21 for pH 5 and pH 11, respectively. The $\beta$ value thus estimated are $4.6 \times 10^{-30}$ esu and $0.6 \times 10^{-30}$ esu, for pH 5(470 nm) and pH 11(420 nm), respectively. Due to the several assumptions introduced in these calculations, the error may be as large as 50%. The estimated $\beta$ value at pH 5 is about eight times higher than the $\beta$ value at pH 11, which is consistent with the observation that the SH intensity is ten times higher at pH 5 compared to the SH intensity at pH 11. Further, the theoretical calculations performed for the C343 molecule (section 3.6), fully support the experimentally measured ratio of $\beta$ values for the protonated and deprotonated forms of the C343 molecule.

### 3.5 Quasi-elastic laser scattering measurements

In order to compare and contrast the above presented adsorption phenomena observed for C343 using SHG at water/DCE interface, we have used the QELS technique to study the adsorption of C343 for different pH values of C343. The typical power spectra of third-order diffracted spot obtained from QELS measurements for neat water/DCE interface and with 0.03mM C343 dissolved in water phase are shown in Fig. 7. For neat water/DCE interface, the frequency of maximum intensity ($f_0$), associated with the mean frequency of the capillary waves was obtained at 6500 Hz. On dissolving 30 μM C343 dye on the water phase, the $f_0$ shifts towards the lower frequency side, indicating a decrease in the interfacial tension caused by the increased number density of the dye molecules adsorbed at the interface. The relationship between the interfacial tension ($\gamma_i$) and $f_0$ is given by the Lamb's equation:[28]

$$f_0 = \frac{1}{2\pi}\sqrt{\frac{\gamma_i k^3}{\rho^w + \rho^{org}}} \quad (11)$$

where $k$ is the capillary wavenumber and $\rho^w$, and $\rho^{org}$ are the densities of water and DCE respectively.

Fig. 8 shows the power spectra of third order diffracted spot obtained from QELS measurements for different pH values of C343 at water/DCE interface. Clearly, on increasing the pH of C343 in water from pH 3 to pH 10, a continuous shift in the frequency of maximum intensity, $f_0$, towards the lower frequency side is observed, reaching lowest for pH 10. On further increasing the pH of the solution, a sudden shift in $f_0$ towards the higher frequency side is observed for pH 11.

The change in frequency reflects the change in the number density of the molecules adsorbed at the interface. The Lower

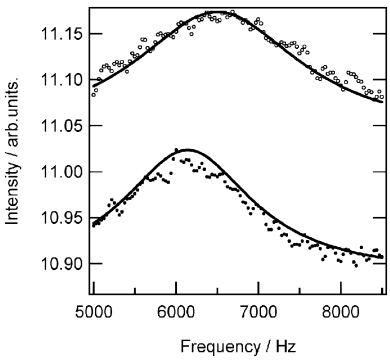


**Fig. 7** Power spectra of third order diffracted spot from the neat water/DCE (open circles) interface and with 30 μM C343 in water phase (filled circles). The solid lines were obtained by least squares curve fitting using a Lorentzian function. The bulk aqueous pH = 5.

 

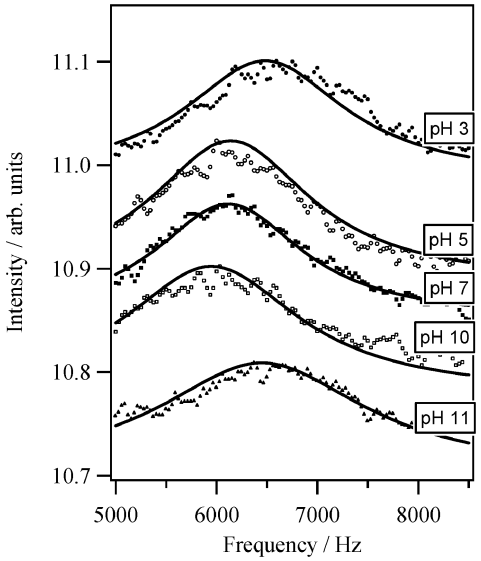


**Fig. 8** Power spectra for different pH values of C343 (30 μM) at water/DCE interface, pH 11 (filled triangles), pH 10 (open squares), pH 7 (filled squares), pH 5 (open circles), pH 3 (filled circles). The solid lines were obtained by least squares curve fitting using a Lorentzian function.

is the frequency or the surface tension; higher is the adsorption at the interface. The QELS data clearly show that the adsorption of C343 molecules is lower at the interface for pH 3 and pH 11, whereas, adsorption is higher for intermediate pH values reaching highest for pH 10. As the SHG intensity is directly proportional to the square of the number of molecules adsorbed per unit area at the interface, the observation of strong adsorption at the intermediate pH values is an indication of strong SHG signal for the intermediate pH values at the interface, and which is indeed the case already discussed above. Thus the QELS data presented above for C343 at water/DCE interface are in very good agreement with the SHG data. As already discussed, the C343 dye molecules at the interface are in H-aggregated form at pH 11 and in both, H-aggregated and J-aggregated form at pH 10. So the sudden decrease in the adsorption of the molecules at the interface at pH 11, compared to the adsorption at pH 10, is due to the change in the aggregation state at the interface.

### 3.6 Theoretical calculations for C343

**3.6.1 Ground-state.** The geometries of the protonated (C343H) and deprotonated (C343-) forms of C343 have been optimized *in vacuo* at the RHF/AM1 level.[29,30] A very detailed analysis of the C343H geometry and $S_0 \rightarrow S_1$ transition energy has already been made by Cave *et al.*[31] They have studied several ground-state protonation conformers of C343. In agreement with their results, we have found that the global minimum for the ground state of the system has hydrogen on the carbonyl, forming an intramolecular hydrogen bond with the nearby carbonyl group.

The neutral form is nearly planar, in the deprotonated form, and the carbonyl ($COO^-$) group is nearly perpendicular to the π-rings. The AM1 ground-state dipole moment of the protonated form ($\mu_g$ = 10.2 D) is in good agreement with experimental one measured in $CHCl_3$ solvent ($\mu_g$ = 9.9 D).[11] The AM1 dipole moment of the deprotonated form is 23.1 D. Both the dipole moment vectors have roughly the same π direction (see Fig. 1).

**3.6.2 Nonlinear properties.** The $\beta_{ijk}$ components of the hyperpolarizability tensor have been computed using two different theoretical methods. First, the sum-over-states theory[32–34] within the INDO/S-CIS framework[35–37] was used. All singlet monoexcited configurations have been taken into account in the configuration interaction. The Nishimoto–Mataga–Weiss formula is used to calculate two-center electron repulsion integrals. The *fr* and *k*-values for Nishimoto–Mataga–Weiss method are 1.2 and 1.0, respectively.[34] Second, the coupled perturbed Hartree–Fock theory[38–40] within the AM1 framework was used. In both the cases, the static electronic vector part of the tensor $\boldsymbol{\beta}$ is calculated using the following equation:

$$\|\beta(0)\| = \left(\sum_i \beta_i^2\right)^{1/2} \text{ with } \beta_i = \sum_j \beta_{ijj} \qquad (12)$$

where *i* and *j* range over the Cartesian coordinates *x*, *y*, *z*. The results are summarised in Table 1. These values should not be taken as "absolute values", as it may be necessary to use an extended basis set in correlated *ab initio* calculations to reach the quantitative results.[41] However, the trends and ratio, $\beta_{\text{protonated}}/\beta_{\text{deprotonated}}$ obtained from these quantum semiempirical methods might be useful in order to compare with the experimental values. The measured values of $\beta$, both for the protonated (at pH = 5) and deprotonated (at pH = 11) forms of C343, are lower compared to the calculated values. However, there is a reasonable agreement between calculated and measured ratio of protonated C343 and deprotonated C343. In all cases, the $\beta$ value of the deprotonated form is rather lower than the protonated one.

An explanation for the lower $\beta$ value for the deprotonated form can be ascribed in terms of electron-donating and electron-withdrawing effects of the carboxy group. Hammett substituent constants $\sigma_p$ and $\sigma_m$ have been split into field/inductive (*F*) and resonance (*R*) parameters according to Swain and Lupton.[42] Values for –COOH, $–COO^-$ and reference substituents ($–NO_2$, $–SiMe_3$)[43] are listed in Table 2.

A high value of *F* means that this substituent is an efficient electron-withdrawing substituent through field effect, whereas, a low value of *F* means that this is an efficient electron-donating substituent through field effect. –COOH and $–COO^-$ $COO^-$ has a very high electron-donating field effect (even greater than $–SiMe_3$) whereas, –COOH has a non-negligible field electron-withdrawing effect.

According to the optimized geometry of deprotonated form of C343 ($C343^-$), the dihedral angle (close to 90°) between the $–COO^-$ group and the rest of the molecule allows no π-conjugation and so no resonance substituent effect. Therefore, $–COO^-$ substituent is a very powerful field electrodonating substituent which leads to a smaller value of $\beta$ and an opposite direction of $\beta$ vector (Fig. 1) for the deprotonated form of C343 molecules.

**Table 1** Calculated and experimental hyperpolarisabilities ($\times 10^{-30}$ esu) of protonated and deprotonated forms of C343

| | $\|\|\beta(0)\|\|_{AM1}$ | $\|\|\beta(0)\|\|_{INDO/S\text{-}CIS}$ | $\beta(0)$, exp. this work | $\beta(0)$ exp. EFISH[11] |
|---|---|---|---|---|
| C343H | 39.8 | 19.8 | 4.6 (pH = 6.5) | 29 ± 2 |
| $C343^-$ | 3.9 | 1.9 | 0.6 (pH = 11) | — |
| $\beta_{\text{protonated}}/\beta_{\text{deprotonated}}$ | 10 | 10 | 8 | — |

**Table 2** Field ($F$) and resonance ($R$) Swain and Lupton substituent constants[41]

| | $F$ | $R$ |
|---|---|---|
| –COOH | 0.34 | 0.11 |
| $–COO^-$ | −0.10 | 0.10 |
| $–NO_2$ | 0.65 | 0.13 |
| $–SiMe_3$ | 0.01 | −0.08 |

## 4. Conclusions

The interfacial properties of C343 dye molecules have been studied at the water/DCE interface using surface sensitive SHG and QELS techniques. The pH dependence of SHG signal from C343 at water/DCE interface shows that for pH 8 and lower, dye adsorbs at the interface in J-aggregated protonated form. At pH 9 and pH 10, the dye is present in both the protonated and deprotonated form at the interface, whereas at pH 11, the dye molecules are present in the H-aggregated deprotonated form at the interface. The $pK_a$ value at the interface is greater than eight, some four units greater than the $pK_a$ of C343 in bulk aqueous solution, and is attributed to the intramolecular hydrogen bonding along with the aggregation of the dye molecules at the interface. The average angle of orientation determined from light polarization measurements for C343 at water/DCE interface for pH 5 and pH 11 are 30° and 42°, respectively. The estimated $\beta$ values at pH 5 and pH 11, are $4.6 \times 10^{-30}$ esu and $0.6 \times 10^{-30}$ esu, respectively, and are consistent with the observed corresponding SH intensities. The QELS data, fully in agreement with SHG data, show that C343 adsorb strongly at the interface when in both, protonated and deprotonated forms at the interface at pH 9 and pH 10, whereas, the adsorption of C343 is weaker when adsorbed only in the deprotonated form at the interface at pH 11. Using two different theoretical frameworks, we find that the calculated ratio of $\beta$ values for protonated and deprotonated forms of C343, are in agreement with the experimentally measured ratio of $\beta$ values. Both, the experimental and calculated $\beta$ value for the deprotonated form is lower than the $\beta$ value for protonated one and is attributed to the electron-donating behavior of $–COO^-$ substituent.

## Acknowledgements

This research work was financed by the office Fédérale de l'Education et de la Science (COST action D15). D.P. thanks Jean Pierre Abid for his support in performing SHG experiments and Dr. Hirohisa Nagatani of Hyogo University of Teacher Education, Japan, for his help in data analysis. Valérie Devaud is acknowledged for her technical assistance.

## References

1 X.-D. Xiao, V. Vogel and Y. R. Shen, *Chem. Phys. Lett.*, 1989, **163**, 555–559.
2 X. Zhao, S. Subrahmanyan and K. B. Eisenthal, *Chem. Phys. Lett.*, 1990, **171**, 558–562.
3 X. Zhao, S. Ong, H. Wang and K. B. Eisenthal, *Chem. Phys. Lett.*, 1993, **214**, 203–207.
4 H. Wang, X. Zhao and K. B. Eisenthal, *J. Phys. Chem. B*, 2000, **104**, 8855–8861.
5 R. R. Naujok, D. A. Higgins, D. G Hanken and R. M. Corn, *J. Chem. Soc., Faraday Trans.*, 1995, **91**, 1411.
6 R. R. Naujok, H. J. Paul and R. M. Corn, *J. Phys. Chem.*, 1996, **100**, 10497–10507.
7 A. A. Tamburello-Luca, Ph. Hebert, R. Antoine, P. F. Brevet and H. H. Girault, *Langmuir*, 1997, **13**, 4428.
8 M. A. Mortazavi, A. Knoesen, S. T. Kowel, R. A. Henry, J. M. Hoover and G. A. Lindsay, *Appl. Phys. B*, 1991, **53**, 287.
9 D. R. Yankelevich, A. Dienes, A. Knoesen, R. W. Schoenlein and C. V. Shank, *IEEE J. Quantum Electron.*, 1992, **28**, 2398.
10 (*a*) S. M. Silence, J. C. Scott, F. Hache, E. J. Ginsburg, P. J. Jenkner, R. D. Miller, R. J. Twieg and W. E. Moerner, *J. Opt. Soc. Am. B*, 1993, **10**, 2306; (*b*) V. Mizrahi and J. E. Sipe, *J. Opt. Soc. Am. B*, 1988, **5**, 661.
11 C. R. Moylan, *J. Phys. Chem.*, 1994, **98**, 13513–13516.
12 A. Piron, P. F. Brevet and H. H. Girault, *J. Electroanal. Chem.*, 2000, **483**, 29.
13 H. Nagatani, A. Piron, P. F. Brevet, D. J. Fermin and H. H. Girault, *Langmuir*, 2002, **18**, 6647.
14 H. Nagatani, Z. Samec, P. F. Brevet, D. J. Fermin and H. H. Girault, *J. Phys. Chem. B*, 2003, **107**, 786–790.
15 P. F. Brevet, *Surface Second Harmonic Generation*, Presses Polytechniques Universitaires Romandes, Lausanne, 1997.
16 H. D. Wang, E. Borguet and K. B. Eisenthal, *J. Phys. Chem. A*, 1997, **101**, 713–718.
17 T. F. Heinz, in *Modern Problems in Condensed Matter Sciences*; ed. H. E. Ponath, G. I. Stegeman, North Holland, Amsterdam, 1991, vol. 29, p. 353.
18 R. E. Riter, E. P. Undiks and N. E. Levinger, *J. Am. Chem. Soc.*, 1998, **120**, 6062–6067.
19 K. Tominaga and G. C. Walker, *J. Photochem. Photobiol. A: Chem.*, 1995, **87**, 127–133.
20 D. Pant and N. E. Levinger, *J. Phys. Chem. B*, 1999, **103**, 7846–7852.
21 T. Katoh, Y. Inagaki and R. Okazaki, *Bull. Chem. Soc. Jpn.*, 1997, **70**, 2279–2286.
22 N. Funaski, *J. Colloid Interface Sci.*, 1977, **60**, 54.
23 M. S. Fernandez and P. Fromherz, *J. Phys. Chem.*, 1977, **81**, 1755.
24 B. Lovelock, F. Grieser and T. W. Healy, *J. Phys. Chem.*, 1985, **89**, 501–507.
25 R. A. Hall, D. Hayes, P. J. Thistlethwaite and F. Grieser, *Colloids Surf.*, 1991, **56**, 339–356.
26 D. Zimdars, J. I. Dadap, K. B. Eisenthal and T. F. Heinz, *J. Phys. Chem. B*, 1999, **103**, 3425–3433.
27 T. Honda, I. Fujii Hirayama, N. Aoyama and A. Miike, *Acta Crystallogr., Sect. C*, 1996, **C52**, 679.
28 H. Lamb, *Hydrodynamics*, Dover, New York, 1945.
29 M. J. S. Dewar, E. G. Zoebisch, E. F. Healy and J. J. P. Stewart, *J. Am. Chem. Soc.*, 1985, **107**, 3902–3909.
30 *Hyperchem 6.03*, HyperCube, Inc. 2000.
31 R. J. Cave and E. W. Castner, *J. Phys. Chem. A*, 2002, **106**, 12117–12123.
32 J. A. Morrell and A. C. Albrecht, *Chem. Phys. Lett.*, 1979, **64**, 46–50.
33 J. F. Ward, *Rev. Mod. Phys.*, 1965, **37**, 1.
34 B. J. Orr and J. F. Ward, *Mol. Phys.*, 1971, **20**, 513.
35 J. E. Ridley and M. C. Zerner, *Theor. Chim. Acta*, 1973, **32**, 111.
36 J. E. Ridley and M. C. Zerner, *Theor. Chim. Acta*, 1976, **42**, 223.
37 *MOS-F V4.2, Semiempirical Molecular Orbital package for Spectroscopy*, Fujitsu, Tokyo, 1999.
38 M. Dupuis and S. Karna, *J. Comput. Chem.*, 1991, **12**, 487.
39 H. A. Kurtz, J. J. P. Stewart and K. M. Dieter, *J. Comput. Chem*, 1990, **11**, 82.
40 J. J. P. Stewart *MOPAC 2000*, Fujitsu, Tokyo, 1999.
41 D. P. Shelton and J. E. Rice, *Chem. Rev.*, 1994, **94**, 3–29.
42 C. G. Swain and E. C. Lupton, *J. Am. Chem. Soc.*, 1968, **90**, 4328–4337.
43 C. Hansch, A. Leo and R. W. Taft, *Chem. Rev.*, 1991, **91**, 165–195.

 